JOURNAL OF MATERIALS SCIENCE 37 (2002) 4361–4368

Oxidation behavior of Si-M-C-O fibers under wide range of oxygen partial pressures

T. SHIMOO, Y. MORISADA, K. OKAMURA
Department of Metallurgy and Materials Science, Graduate School of Engineering, Osaka Prefecture University, 1-1, Gakuen-cho, Sakai, 599-8531 Osaka, Japan

The active-to-passive oxidation transition for three types of Si-M-C-O fibers (Lox M, ZMI and SA) was examined at 1773 K and $p_{O_2} = 1$–25000 Pa through TG, XRD analysis, SEM observation and tensile tests. The p_{O_2} value of the active-to-passive oxidation transition for Lox M and ZMI fibers was between 100–250 Pa. While the strength of Lox M and ZMI fibers was considerably retained after passive-oxidation, it was markedly degraded after active-oxidation ($\sigma \fallingdotseq 0$ Gpa). For SA fibers, the passive-oxidation occurred even at $p_{O_2} = 1$ Pa, producing a very large decrease in the tensile strength.

1. Introduction

Polycarbosilane-derived silicon carbide fibers are of a great importance as a reinforcing material in ceramic-matrix composites for high-temperature applications [1]. The composites are often employed in oxidizing environments with different oxygen potentials. Therefore, a deep understanding of the oxidation behavior of silicon carbide fibers in such circumstances is of both practical and basic interest. Silicon carbide fibers display the quite different oxidation behaviors, depending on the oxygen potential of atmospheres. There are many researches on the passive-oxidation of the silicon carbide fibers in oxidizing environments with higher oxygen potentials, such as H_2-H_2O, CO_2, air, Ar-O_2 and O_2 [2–19]. The passive-oxidation leads to the formation of a protective silica film, protecting the fibers from further oxidation. In addition, the silica film suppresses the thermal decomposition of an amorphous silicon oxycarbide phase in the silicon carbide fibers. Consequently, the tensile strength of the silicon carbide fibers was considerably retained after the passive-oxidation. On the other hand, the silicon carbide fibers seems to be subjected to serious damage by the active-oxidation at lower oxygen potentials, as well as silicon carbide ceramics. However, an investigation has been little performed on the active-oxidation of silicon carbide fibers [8].

Present authors were studied the oxidation behaviors of Si-C-O fibers such as Nicalon, Hi-Nicalon and Hi-Nicalon S (Nippon Carbon Co., Tokyo, Japan) at 1773 K and $p_{O_2}1 = 1$–100000 Pa [20, 21]. The oxygen partial pressure for the active-to-passive oxidation transition decreased in the following order: $p_{O_2} = 100$–250 Pa for Nicalon, $p_{O_2} = 10$–25 Pa for Hi-Nicalon and $p_{O_2} = 1$–2.5 Pa for Hi-Nicalon S. The strength of both Nicalon and Hi-Nicalon was seriously degraded after active-oxidation ($\sigma \fallingdotseq 0$ GPa), though it was considerably retained after passive-oxidation. On the other hand, Hi-Nicalon S having a nearly stoichiometric composition was held to $\sigma \fallingdotseq 1$ GPa even after active-oxidation.

Compared to Si-C-O fibers, Si-M-C-O fibers such as Lox M, ZMI and SA (Ube Industries Co., Tokyo, Japan) show considerable difference in their composition and microstructure. Particularly noteworthy is the presence of a slight amounts of metallic elements in Si-M-C-O fibers: M = Ti for Lox M fibers, M = Zr for ZMI fibers and M = Al for SA fibers. Therefore, a large difference of the oxidation behavior between Si-C-O and Si-M-C-O fibers can be expected. In the present work, the oxidation tests of three types of Si-M-C-O fibers were performed at 1773 K in Ar-O_2 gas mixtures with $p_{O_2} = 1$–25000 Pa. The active-to-passive oxidation transition and its effect on the mechanical properties of the fibers were investigated in detail. In addition, the oxidation behavior of Si-M-C-O fibers was compared with that of Si-C-O fibers [20, 21].

2. Experimental method

The materials employed in this study are polycarbosilane-derived Si-M-C-O fibers (Ube Industries Co., Tokyo, Japan): Lox M (M = Ti), ZMI (M = Zr) and SA-3 grade (M = Al) fibers. Table I shows the composition of Si-M-C-O fibers, together with those of Si-C-O fibers such as Nicalon, Hi-Nicalon and Hi-Nicalon S fibers (Nippon carbon Co., Tokyo, Japan) [22–24]. While both Lox M and ZMI contain a large amount of oxygen and a large excess of carbon, SA contains a only slight amount of oxygen and excess carbon (a nearly stoichiometric composition).

The oxidation tests of the fibers were conducted as follows: 500 mg of fibers, 30 mm in length were placed in a platinum crucible and then were heat-treated in an alumina tube of a vertical SiC resistance furnace for 20 h at 1773 K in Ar-O_2 gas mixture with each oxygen partial pressure from 1 to 25000 Pa. The Ar-O_2 gas mixture was allowed to flow into the alumina tube at a flow rate

TABLE I Composition of polycarbosilane-derived silicon carbide fibers

	Lox M	ZMI	SA	Nicalon	Hi-Nicalon	Hi-Nicalon S
Chemical composition						
Si (mass%)	55.4	56.6	67	58.6	62.4	68.9
C (mass%)	32.4	34.8	31	31.7	37.1	30.9
O (mass%)	10.2	7.6	<1.0	11.7	0.5	0.2
Ti (mass%)	2.0	–	–	–	–	–
Zr (mass%)	–	1.0	–	–	–	–
Al (mass%)	–	–	<1.0	–	–	–
Si/C atomic ratio	1.37	1.44	1.08	1.31	1.39	1.05

of 8.33×10^{-6} m^3/s. During heat-treatment, the mass change of the fibers was determined by a digital-type automatic recording balance. Upon completion of the heat-treatment, the fibers were quenched by raising the crucible to the lower temperature zone of the furnace.

The fibers after heat-treatment were subjected to X-ray diffraction (XRD) analysis, scanning electron microscopic (SEM) observation and tensile tests. The crystal phases of the fibers were identified with an X-ray diffractometer (Rigaku Co., Type RINT 1100, Tokyo, Japan) using Cu Kα radiation, and the apparent size of β-SiC crystallite was calculated from the half-value width of (111) peak using Scherrer's formula. The fiber morphologies were examined using a field emission scanning electron microscope (Hitachi Ltd., Type S5400, Tokyo, Japan). Tensile tests were conducted for the fibers from which the silica film was removed with $NH_4F + HF$ solution. The room-temperature tensile strength of a fiber of 10 mm length was determined using a universal tensile tester (Orientec Co., Type TENSILON UTM-II-20. Tokyo, Japan) with a load cell of 4.9 N and a crosshead speed of 2 mm/min. The mean value for 20 measurements was taken as the tensile strength of each fiber.

3. Result

3.1. TG curves

Figs 1, 2 and 3 show the TG curves of Lox M, ZM and SA fibers heated at 1773 K and in Ar-O_2 gas mixtures of different oxygen partial pressures (p_{O_2}). Here,

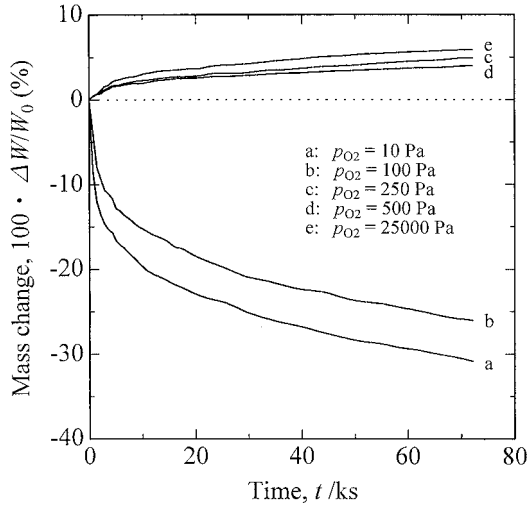

Figure 1 TG curves for Lox M fibers heated at 1773 K in Ar-O_2 gas mixtures with different oxygen partial pressures.

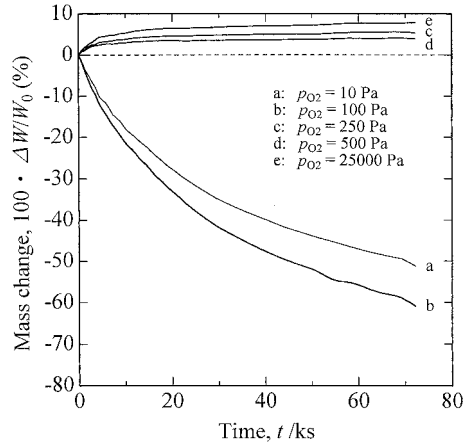

Figure 2 TG curves for ZMI fibers heated at 1773 K in Ar-O_2 gas mixtures with different oxygen partial pressures.

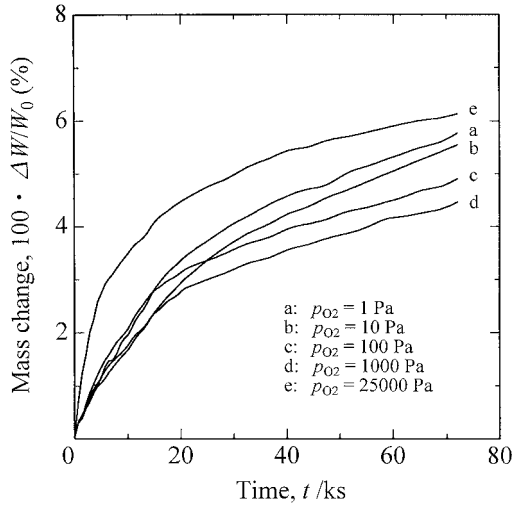

Figure 3 TG curves for SA fibers heated at 1773 K in Ar-O_2 gas mixtures with different oxygen partial pressures.

ΔW and W_0 are the mass change value determined by thermogravimetry (TG), and the initial mass of the fibers, respectively. The effect of p_{O_2} on TG curve is complicated, as well as Nicalon, Hi-Nicalon and Hi-Nicalon S [20, 21]. The mass gain at $p_{O_2} \geqq 250$ Pa and the mass loss at $p_{O_2} \leqq 100$ Pa are observed for Lox M and ZMI fibers. On the other hand, for SA fibers, only the mass gain was caused by the heat-treatment under present experimental condition (at 1773 K and $p_{O_2} = 1$–25000 Pa). The mass gain is due to the passive-oxidation of the SiC crystallites in the fibers, whereas the mass loss is due to both thermal decomposition of SiC_XO_Y phase and active-oxidation of SiC crystallites [20, 21].

3.2. X-ray diffraction data

Fig. 4 shows the X-ray diffraction patterns of Lox M fibers. The as-received fibers have a broad X-ray diffraction pattern of β-SiC, implying that Lox M fibers are in the amorphous or nano-crystalline state. The broad peaks of β-SiC at $2\theta \fallingdotseq 60$ and 72° after oxidation at $p_{O_2} \geqq 250$ Pa indicate that the fibers are still in the nano-crystalline state. The oxidation at $p_{O_2} = 10$ and 100 Pa caused a significant growth of β-SiC crystals. It may be noted that a sharp cristobalite peak at $2\theta \fallingdotseq 20°$ was found in all the fibers oxidized at $p_{O_2} = 10$–25000 Pa. In particular, the presence of cristobalite in the fibers oxidized at $p_{O_2} = 10$ and 100 Pa is in seemingly conflict with the occurrence of active-oxidation characterized by a mass loss (Fig. 1).

Fig. 5 shows the X-ray diffraction patterns of ZMI fibers. The as-received fibers are in the nano-crystalline state for β-SiC, as well as Lox M fibers. The fibers oxidized at $p_{O_2} \geqq 250$ Pa were coated with cristobalite film and preserved a nano-crystalline structure. The oxidation at $p_{O_2} \leqq 100$ Pa caused a significant cry-atallization of β-SiC. From this result and a great mass loss (Fig. 2), it is evident that ZMI fibers underwent thermal-decomposition and subsequent active-oxidation at $p_{O_2} \leqq 100$ Pa.

Fig. 6 shows the X-ray diffraction patterns of SA fibers. The very sharp diffraction peaks of β-SiC show that SA fibers are highly crystalline even in the as-received state. The oxidation at lower oxygen partial pressures caused gradual crystallization of β-SiC. A cristobalite film was formed on all the fibers exposed at $p_{O_2} = 1$–25000 Pa. Obviously, by considering a mass gain in TG curve (Fig. 3), SA fibers were oxidized in the passive-oxidation regime even at $p_{O_2} = 1$ Pa.

The apparent β-SiC crystallite size (D_{SiC}) was calculated from the half-value width of the diffraction peak at $2\theta = 60°$, using Scherrer's formula. The value of D_{SiC} was shown in Fig. 7. For Lox M and ZMI fibers, the crystal growth was little observed at $p_{O_2} \geqq 250$ Pa, i.e., in the passive-oxidation region. There was a significant coarsening of β-SiC crystals in the active-oxidation region at $p_{O_2} \leqq 100$ Pa. Even in the as-received state, SA fibers have a significantly coarsened-grain, the size of which was outside the limits of the application of Scherrer's formula. For comparison with other fibers, the calculated values are shown in Fig. 7. β-SiC crystallite size of SA fibers appears to be little dependent on p_{O_2}.

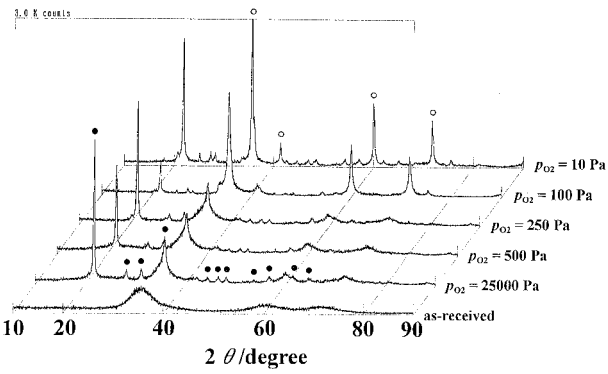

Figure 4 XRD patterns for Lox M fibers heated for 20 h at 1773 K in Ar-O_2 gas mixtures with different oxygen partial pressures. ○: β-SiC, ●: cristobalite.

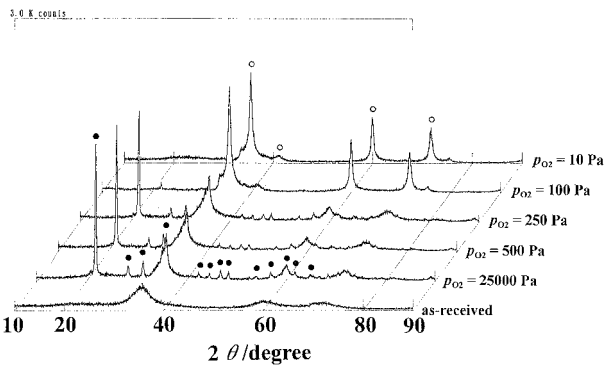

Figure 5 XRD patterns for ZMI fibers heated for 20 h at 1773 K in Ar-O_2 gas mixtures with different oxygen partial pressures. ○: β-SiC, ●: cristobalite.

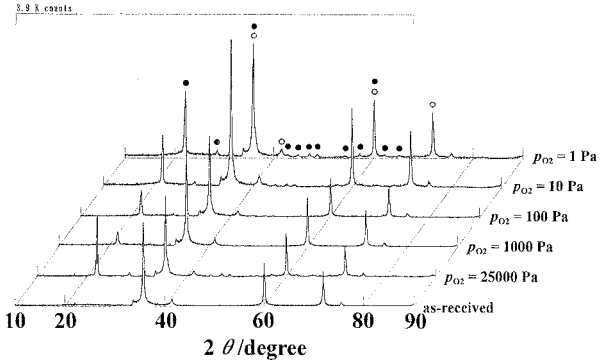

Figure 6 XRD patterns for SA fibers heated for 20 h at 1773 K in Ar-O_2 gas mixtures with different oxygen partial pressures. ○: β-SiC, ●: cristobalite

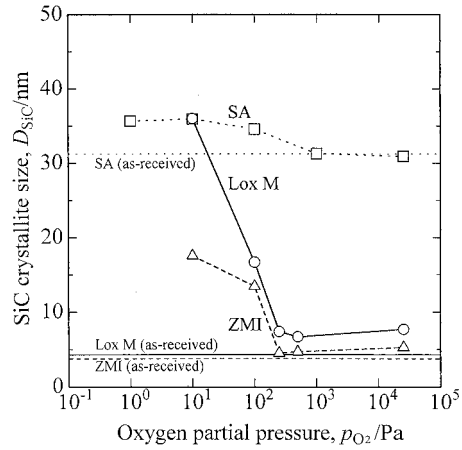

Figure 7 Relationship between β-SiC crystallite size and oxygen partial pressure for fibers heated for 20 h at 1773 K in Ar-O_2 gas mixtures.

3.3. Fiber morphologies

The surface and cross section of Lox M, ZMI and SA fibers after oxidation are shown in Figs 8, 9 and 10, respectively. As can be seen from the mass gain and the strong XRD peaks of cristobalite, Lox M and ZMI fibers were passively oxidized at $p_{O_2} = 250$ Pa (Figs 1, 2, 4 and 5). Therefore, Figs 8 and 9 show that a cracked film of cristobalite was formed on the fibers. A large increase in the volume of cristobalite was caused by the

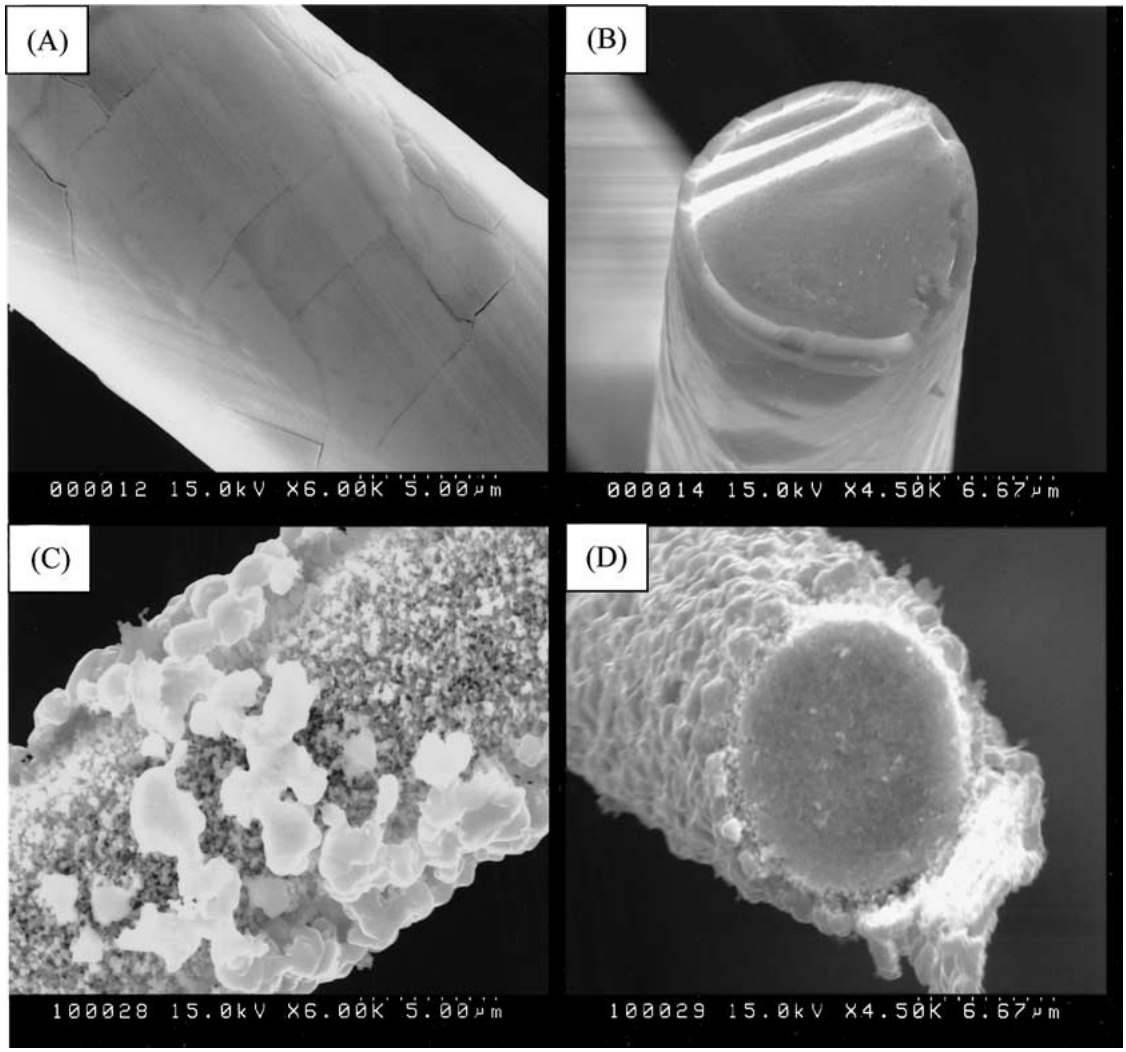

Figure 8 SEM photographs for Lox M fibers heated for 20 h at 1773 K and $p_{O_2} = 250$ Pa (A, B) and 10 Pa (C, D).

β-to-α transformation at about 500 K, resulting in the formation of the cracks during quenching of the oxidized fibers. In addition, as can be seen from photos (B), the core of both fibers had a pore-free and glassy appearance. The active-oxidation of Lox M and ZMI fibers at $p_{O_2} = 10$ Pa is clearly proved by a significant mass loss and the absence of cristobalite peaks (Figs 1, 2, 4 and 5). For Lox M fibers after oxidation at $T = 1773$ K and $p_{O_2} = 10$ Pa, large β-SiC grains were formed on the fiber surface and the fiber core has a porous and coarse-grained structure (C and D). Such a dual structure was observed in Nicalon fibers after the active-oxidation [20]. As shown in Fig. 9C and D, ZMI fibers had not the dual structure, and yet they were porous throughout the entire area from the surface to the core of the fibers. SA fibers, as a consequence of the passive-oxidation, were coated with a very thick and cracked cristobalite film after exposure at $T = 1773$ K and $p_{O_2} = 10$ Pa (Fig.10 A and B). Further development of SiO_2 film was found at $p_{O_2} = 1$ Pa (Fig. 10C and D), being consistent with TG and XRD data (Figs. 3 and 6). The presence of large gas-bubbles implies that the reaction occurred at the SiO_2-film/core interface. In addition, the appearance of gas-bubbles shows the softening of SiO_2 film during oxidation at 1773 K (D).

3.4. Tensile strength

Fig. 11 shows the room-temperature tensile strength (σ) of the fibers oxidized at $T = 1773$ K and different oxygen partial pressures. Tensile tests were conducted on the fibers after having removed the SiO_2 film (unoxidized cores). In the passive-oxidation region at $p_{O_2} \geqq 100$ Pa, the retained strengths of Lox M and ZMI fibers were 26–37% and 35–43% of the strength in the as-received state, respectively. The active-oxidation at $p_{O_2} = 10$ Pa produced a significant degradation of strength of both Lox M and ZMI fibers ($\sigma \fallingdotseq 0$ GPa). On the other hand, SA fibers were too fragile to be subjected to a tensile test regardless of the heat-treatment in the passive-oxidation region.

4. Discussion

Polycarbosilane-derived silicon carbide fibers are principally composed of β-SiC crystallite, free carbon and an amorphous SiC_XO_Y phase. Lox M and ZMI fibers contain 10.3 and 7.8 mass% O as an amorphous silicon oxycarbide (SiC_XO_Y) phase, respectively. The exposure at the experimental temperature (1773 K) causes the thermal decomposition of SiC_XO_Y phase: the crystallization into β-SiC and the generation of SiO and CO

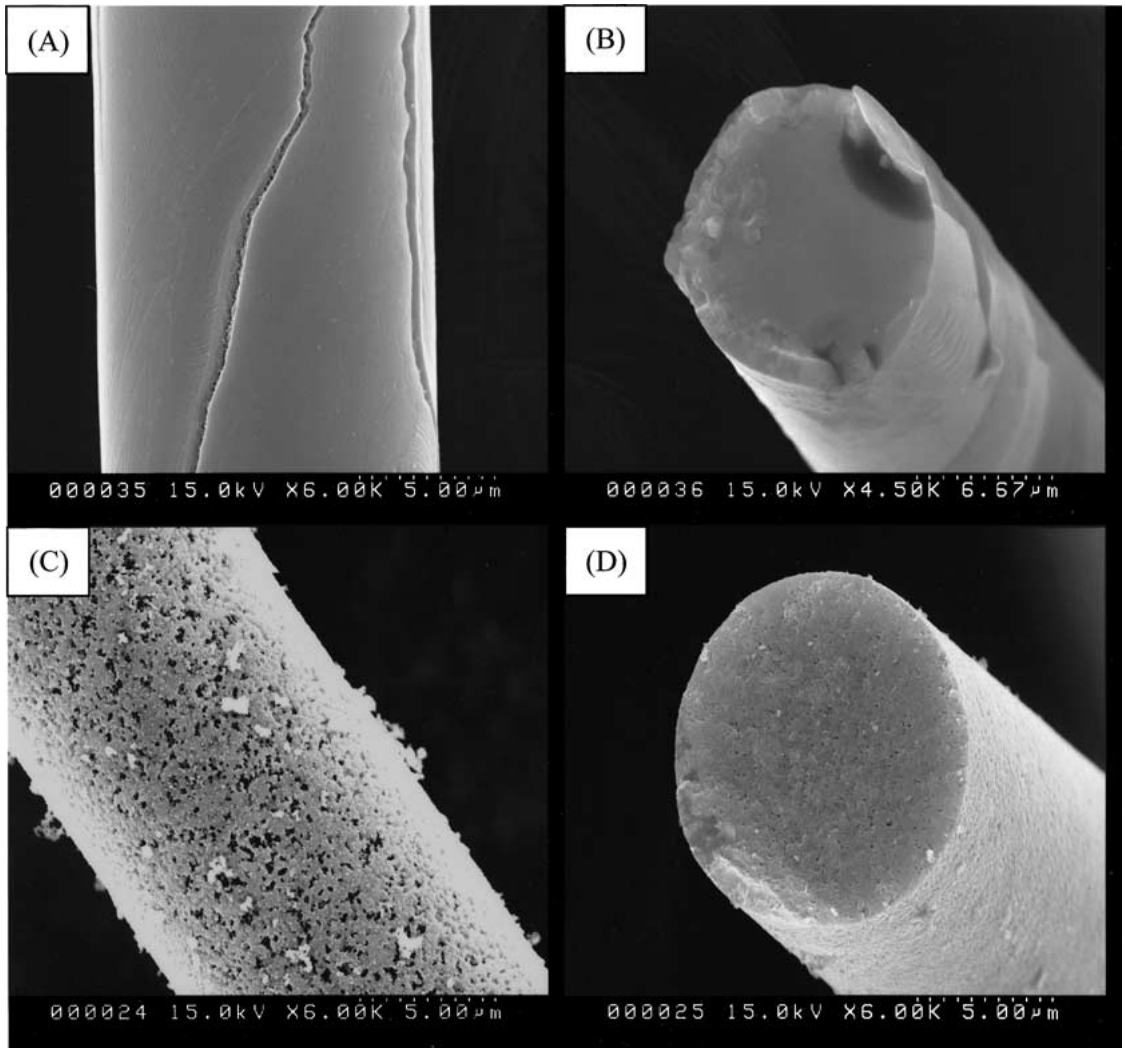

Figure 9 SEM photographs for ZMI fibers heated for 20 h at 1773 K and $p_{O_2} = 250$ Pa (A, B) and 10 Pa (C, D).

gases. In addition, a large excess carbon is present in both fibers as free carbon: C/Si (atomic ratio) = 1.37 for Lox M fibers and 1.44 for ZMI fibers. While the thermal decomposition of SiC_XO_Y phase and the oxidation of free carbon yield mass loss, the passive-oxidation of β-SiC crystallites yields mass gain. For SA fibers, the mass loss caused by the thermal decomposition of SiC_XO_Y phase and the oxidation of free carbon is of little significance, owing to a slight amount of oxygen (<1 mass%) and free carbon (C/Si = 1.08). Finally, the passive-oxidation of Lox M, ZMI and SA fibers causes a mass gain, according to the following overall reactions:

for Lox M fibers:

$$SiTi_{0.02}C_{1.37}O_{0.32}(s) + 2.23O_2(g) = SiO_2(s) + 0.02TiO_2(s) + 1.37CO_2(g) \quad (1)$$

$$SiTi_{0.02}C_{1.37}O_{0.32}(s) + 1.545O_2(g) = SiO_2(s) + 0.02TiO_2(s) + 1.37CO(g) \quad (2)$$

$$SiTi_{0.02}C_{1.37}O_{0.32}(s) + 0.86O_2(g) = SiO_2(s) + 0.02TiO_2(s) + 1.37C(g) \quad (3)$$

for ZMI fibers:

$$SiZr_{0.01}C_{1.44}O_{0.24}(s) + 2.33O_2(g) = SiO_2(s) + 0.01ZrO_2(s) + 1.44CO_2(g) \quad (4)$$

$$SiZr_{0.01}C_{1.44}O_{0.24}(s) + 1.61O_2(g) = SiO_2(s) + 0.01ZrO_2(s) + 1.44CO(g) \quad (5)$$

$$SiZr_{0.01}C_{1.44}O_{0.24}(s) + 0.89O_2(g) = SiO_2(s) + 0.01ZrO_2(s) + 1.44C(g) \quad (6)$$

for SA fibers:

$$SiAl_{0.02}C_{1.08}O_{0.03}(s) + 2.10O_2(g) = SiO_2(s) + 0.01Al_2O_3(s) + 1.08CO_2(g) \quad (7)$$

$$SiAl_{0.02}C_{1.08}O_{0.03}(s) + 1.56O_2(g) = SiO_2(s) + 0.01Al_2O_3(s) + 1.08CO(g) \quad (8)$$

$$SiAl_{0.02}C_{1.08}O_{0.03}(s) + 1.02O_2(g) = SiO_2(s) + 0.01Al_2O_3(s) + 1.08C(s) \quad (9)$$

Here, it was assumed that SA fibers contain 1 mass% Al and 1 mass% O (maximum values in Table 1). Which reaction occurs is strongly dependent upon the oxygen

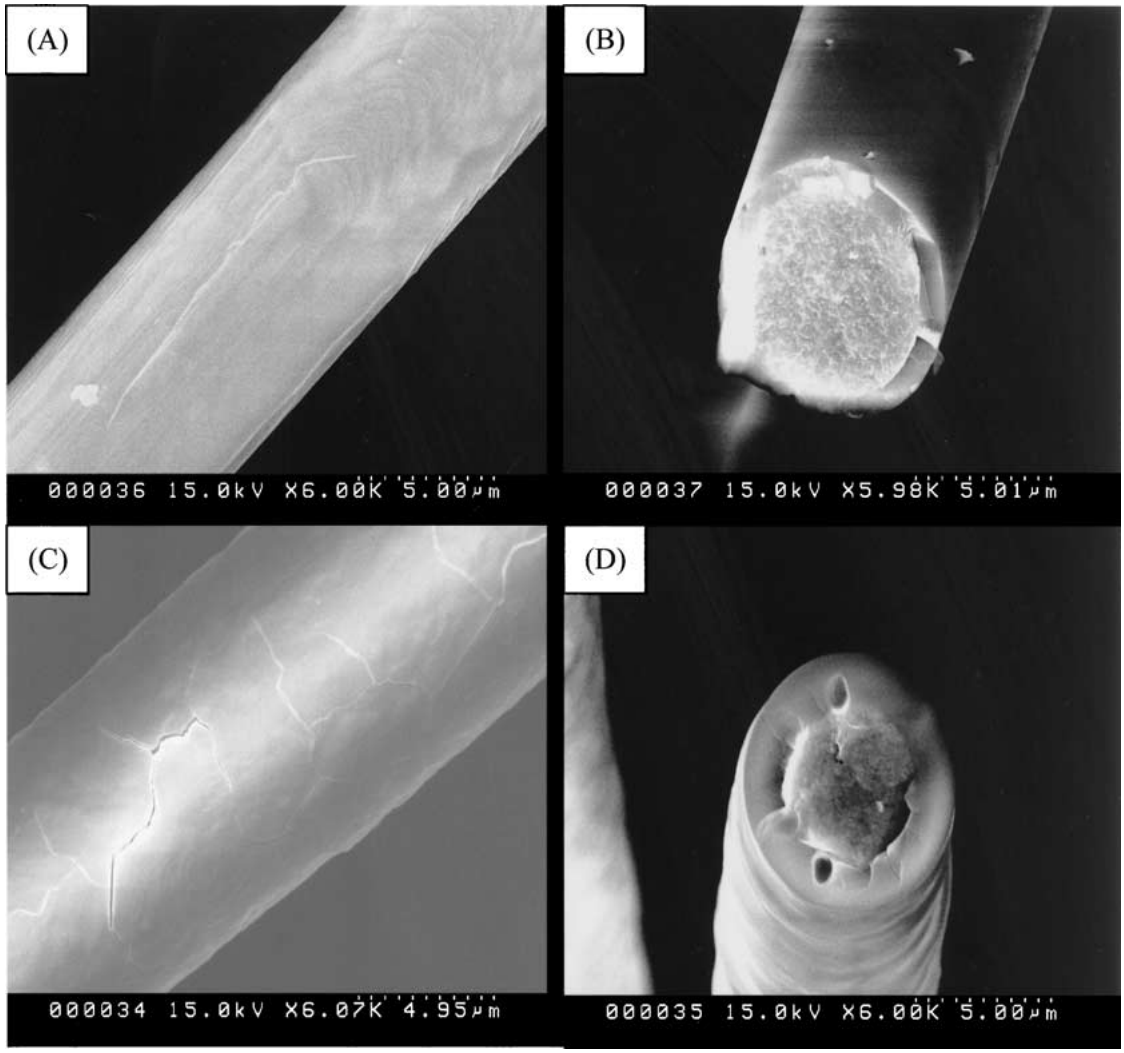

Figure 10 SEM photographs for SA fibers heated for 20 h at 1773 K and $p_{O_2} = 10$ Pa (A, B) and 1 Pa (C, D).

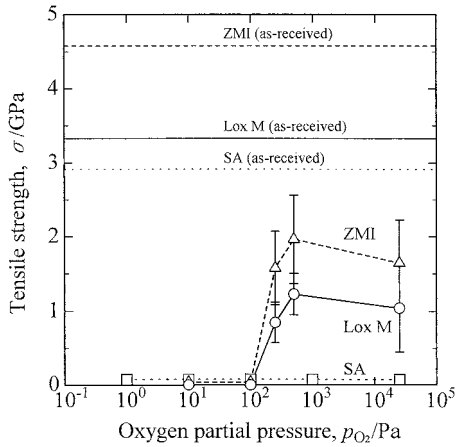

Figure 11 Relationship between room-temperature tensile strength and oxyen partial pressure for fibers heated for 20 h at 1773 K in Ar-O_2 gas mixtures.

potential of oxidizing environment. As can be seen from TG measurement, XRD analysis and SEM observation, the passive-oxidation occurred at $p_{O_2} \geqq 250$ Pa for both Lox M and ZMI fibers but it occurred even at 1 Pa for SA fibers.

The complete decomposition of SiC_XO_Y phase yielded the following mass loss: $100 \cdot \Delta W / W_0 = 20.5$ for Lox M fibers and 13.5 for ZMI fibers [22]. TG data shows that the mass losses of both fibers were much greater than the above values at $p_{O_2} \leqq 100$ Pa. This exhibits that the active-oxidation of β-SiC crystallites by O_2 gas occurred after completion of the thermal decomposition of SiC_XO_Y phase. On the other hand, SA fibers were not actively oxidized under the experimental conditions. The overall reactions for the active-oxidation of Lox M and ZMI fibers are given by the following equations:

for Lox M fibers:

$$SiTi_{0.02}C_{1.37}O_{0.32}(s) + 1.73O_2(g) = SiO(g) + 0.02TiO_2(s) + 1.37CO_2(g) \quad (10)$$

$$SiTi_{0.02}C_{1.37}O_{0.32}(s) + 1.045O_2(g) = SiO(g) + 0.02TiO_2(s) + 1.37CO(g) \quad (11)$$

$$SiTi_{0.02}C_{1.37}O_{0.32}(s) + 0.36O_2(g) = SiO(g) + 0.02TiO_2(s) + 1.37C(g) \quad (12)$$

for ZMI fibers:

$$SiZr_{0.01}C_{1.44}O_{0.24}(s) + 1.83O_2(g) = SiO(s) + 0.01ZrO_2(s) + 1.44CO_2(g) \quad (13)$$

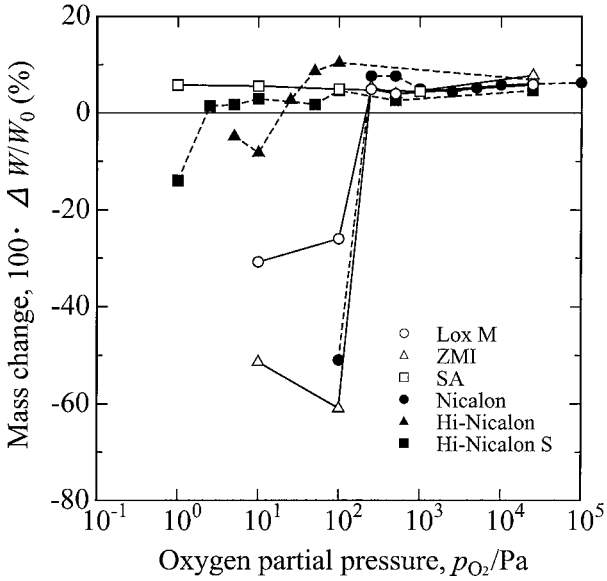

Figure 12 Relationship between mass change and oxygen partial pressure for fibers heated for 20 h at 1773 K in Ar-O_2 gas mixtures.

$$SiZr_{0.01}C_{1.44}O_{0.24}(s) + 1.11O_2(g) = SiO(s) + 0.01ZrO_2(s) + 1.44CO(g) \quad (14)$$

$$SiZr_{0.01}C_{1.44}O_{0.24}(s) + 0.39O_2(g) = SiO(s) + 0.01ZrO_2(s) + 1.44C(g) \quad (15)$$

Fig. 12 shows the mass change of fibers for 72 ks at 1773 K, as a function of the oxygen partial pressure, p_{O_2}. The mass changes of Si-C-O fibers (Nicalon, Hi-Nicalon and Hi-Nicalon S) also are shown for comparison with those of Si-M-C-O fibers [20, 21]. In the passive-oxidation region, the decrease in oxygen partial pressure retarded the mass gain at $p_{O_2} \geqq 500$ Pa and enhanced the mass gain at $p_{O_2} \leqq 500$ Pa. This seems to be because the type of oxidation reaction was changed by the reduction in p_{O_2}. For example, with decreased p_{O_2} value, the reaction for the passive-oxidation of Lox M fibers may vary in this order: Equations 1–3. This is verified by the result that the oxidation at $p_{O_2} = 500$ Pa resulted in the formation of an intermediate carbon layer between the cristobalite film and the unoxidized core of Nicalon [20]. Both Lox M and ZMI fibers caused a marked mass loss at $p_{O_2} \leqq 100$ Pa, as well as Nicalon fibers. Therefore, the oxygen partial pressure of the active-to-passive oxidation transition, $p_{O_2^*}$, for these fibers is between 100 and 250 Pa. Such a apparently high $p_{O_2^*}$ value may be responsible for a large amount of oxygen (SiC_XO_Y phase) and free carbon existing in the fibers (Table 1). Firstly, the generation of SiO and CO gases, as a consequence of the thermal decomposition of SiC_XO_Y phase and the oxidation of free carbon, leads to the reduction of a p_{O_2} value on the fiber surface. Secondly, the oxidation of SiO and CO gases at lower temperatures reduce a p_{O_2} value of the gas that is fed into the reaction tube. Thus Lox M, ZMI and Nicalon were actively oxidized at a relatively high oxygen partial pressure ($p_{O_2} = 100$ Pa). Hi-Nicalon contains a large amount of free carbon though it contains a slight of oxygen, i.e., 0.5% O. Hi-Nicalon S has a nearly stoichiometric composition (C/Si = 1.05), in addition to still lower oxygen content (0.2% O). Consequently, the $p_{O_2^*}$ value decreased as follows: 10–25 Pa for Hi-Nicalon and 1–2.5 Pa for Hi-Nicalon S. SA is a nearly stoichiometric SiC fiber which contains a slight of oxygen (<1 mass%), as well as Hi-Nicalon S fibers. However, SA fibers were passively oxidized even at $p_{O_2} = 1$ Pa.

There is a wide range of active-to-passive oxidation transition domain in the oxidation of silicon carbide [25]. For example, the active-to-passive oxidation transition domain is between 1.6×10^{-4}–820 Pa at 1773 K. The gas bubbles may be formed by not only the thermal decomposition of SiC_XO_Y phase but also by the interaction of the SiO_2 film with the fiber core. Therefore, whether the SiO_2 film is proof of the pressure of gas bubbles is thought to be critical of the oxidation behavior the fibers. The formation of SiO_2 film on the fiber surface and of gas bubbles (SiO and CO) in the SiO_2 film are thought to occur concurrently in the active-to-passive oxidation transition domain. While the active-oxidation is caused by the breaking of SiO_2 film, the passive-oxidation is allowed to continue by the condensation of SiO gas into SiO_2. The breaking of SiO_2 film is attributed to no resistance to the pressure of gas bubbles. On the other hand, the condensation of SiO gas is caused by oxygen which diffuses into gas bubbles through the SiO_2 film.

The passive-oxidation of SA fibers at $p_{O_2} = 1$ Pa appears to be attributable to the presence of a minute of aluminum. Alumina, as a oxidation product of aluminum, reacts with the SiO_2 film to form an alumino-silicates. At 1773 K, the softening of the alumino-silicate film was observed because of low melting point (Fig. 10D). The alumino-silicates have a high oxygen permeability, presumably enhancing the passive-oxidation of the fibers [26, 27]. Such development of SiO_2 film showed a high degree resistance to the pressure of gas bubbles, resulting in suppression of the active-oxidation of SA fibers even at $p_{O_2} = 1$ Pa. On the other hand, the oxidation of Hi-Nicalon S fibers, having a nearly stoichiometric composition but being free from aluminum, was sluggish compared to SA fibers. For example, the mass gains ($100 \cdot \Delta W/W_0$) at $T = 1773$ K and $p_{O_2} = 10$ Pa are +5.54% for SA fibers and +2.90% for Hi-Nicalon S fibers [21]. Different oxidation rates may be partly responsible for difference in the specific surface area of fibers. Hi-Nicalon S fibers of 12 μm diameter should be more slowly oxidized than SA fibers of 10 μm diameter. Finally, thin SiO_2 film of Hi-Nicalon S fibers was not proof of the pressure of gas bubbles, causing the active-oxidation at $p_{O_2} = 1$ Pa. The SiO_2 film of Nicalon, Hi-Nicalon, Hi-Nicalon S and ZMI fibers finally disappeared after active oxidation, even if it was initially formed. On the other hand, XRD analysis shows that the cristobalite phase was present in Lox M fibers after active-oxidation (Fig. 4). The titanium-containing silica film is thought to be retained after active-oxidation, owing to difficulty in reducing.

As mentioned above, Lox M and ZMI fibers were actively oxidized as well as Nicalon fibers. The thermal decomposition of SiC_XO_Y phase could not be

suppressed owing to the absence of SiO_2 film. In addition, the active-oxidation of SiC grains caused an increase in porosity of the fibers, resulting in a marked degradation of the strength ($\sigma \fallingdotseq 0$ GPa). For Lox M and ZMI fibers with high oxygen content, the strength was considerably degraded in the passive-oxidation region. This is probably attributed to the thermal decomposition of SiC_XO_Y phase before the formation of continuous SiO_2 film, as well as Nicalon fibers [20]. However, 30–40% of the strength in the as-received state was retained. SA fibers became significantly fragile after passive-oxidation ($\sigma \fallingdotseq 0$ GPa), though they have a nearly stoichiometric composition, as well as Hi-Nicalon S fibers having a strength of 1 GPa after active-oxidation. The strength of SA fibers was degraded to $\sigma \fallingdotseq 0.6$ GPa even after heat-treatment at 1773 K under argon atmosphere. This shows that the heat-treatment at 1773 K causes a great degradation of strength, irrespective of the p_{O_2} value of environments. Excessive oxidation of SA fibers seems to produce imperfections, leading to further drop of strength (finally $\sigma \fallingdotseq 0$ GPa).

5. Conclusion

Three types of Si-M-C-O fibers such as Lox M, ZMI and SA were oxidized at 1773 K in Ar-O_2 gas mixtures with $p_{O_2} = 1$–25000 Pa.

The active-to-passive oxidation transition was found at $p_{O_2} = 100$–250 Pa for both Lox M and ZMI fibers. The passive-oxidation caused the formation of a cristobalite film on the fibers. The decrease in oxygen partial pressure at $p_{O_2} \leqq 500$ Pa enhanced the mass gain in the passive-oxidation region. The fibers oxidized in the active-oxidation regime showed a significant coarsening of SiC crystals and a marked increase in porosity. While 30–40% of the strength in the as-received state was retained after passive-oxidation, the strength was significantly degraded after active-oxidation ($\sigma \fallingdotseq 0$ GPa). For SA fibers, the passive-oxidation took place even at $p_{O_2} = 1$ Pa, resulting in a significant development of cristobalite film. In addition, all the oxidized fibers were too fragile to be subjected to tensile test.

Acknowledgement

This study was partly supported by a grant from the Ministry of Education, Science, Sports and Culture under Grant No. 11450255.

References

1. R. R. NASLAIN, *Adv. Composite Mater.* **8** (1999) 3.
2. Y. MANIETTE and A. OBERLIN, *ibid.* **24** (1989) 3361.
3. L. FILLIPUZZI and R. NASLAIN, in Proc. 7th CIMTEC (Elsevier, Amsterdam, 1991) p. 35.
4. H. E. KIM and A. J. MOORHEAD, *J. Amer. Ceram. Soc.* **74** (1991) 666.
5. T. SHIMOO, H. CHEN and K. OKAMURA, *J. Ceram. Sc. Jpn* **100** (1992) 929.
6. T. SHIMOO, T. HAYATSU, M. TAKEDA, H. ICHIKAWA, T. SEGUCHI and K. OKAMURA, *ibid.* **102** (1994) 617.
7. M. H. BERGER, N. HOCHET and A. R. BUNSELL, *J. Microsc.* **177** (1995) 230.
8. P. LE. COUSTUMER, M. MONTHIOUX and A. OBERLIN, *Br. Ceram. Trans.* **94** (1995) 177.
9. G. CHOLLON, R. R. PAILLER, R. NASLAIN, F. LAANANI, M. MONTHIOUX and P. OLRY, *J. Mater. Sci.* **32** (1997) 327.
10. G. CHOOLLON, M. CZEERNIAK, R. PAILLER, X. BOURRA, R. NASLAIN, J. P. PILLOT and R. CANNET, *ibid.* **32** (1997) 893.
11. M. H. BERGER, N. HOCHET and A. R. BUNSELL, *J. Microsc.* **185** (1997) 243.
12. T. SHIMOO, F. TOYODA and K. OKAMURA, *J. Ceram. Soc. Jpn* **106** (1998) 447.
13. Y. T. ZHU, S. T. TAYLOR, M. G. STOUT, D. P. BUTT and T. C. LOWE, *J. Amer. Ceram. Soc.* **81** (1998) 655.
14. T. SHIMOO, F. TOYODA and K. OKAMURA, *J. Ceram. Soc. Jpn* **107** (1999) 263.
15. M. TAKEDA, J. SAKAMOTO, Y. IMAI and H. ICHIKAWA, *Composites Sci. Tech.* **59** (1999) 813.
16. T. SHIMOO, F. TOYODA and K. OKAMURA, *J. Mater. Sci.* **35** (2000) 3301.
17. *Idem.*, *J. Amer. Ceram. Soc.* **83** (2000) 1450.
18. *Idem.*, *J. Mater. Sci.* **35** (2000) 3811.
19. T. SHIMOO, H. TAKEUCHI, M. TAKEDA and K. OKAMURA, *J. Ceram. Soc. Jpn* **108** (2000) 1096.
20. T. SHIMOO, Y. MORISADA and K. OKAMURA, *J. Amer. Ceram. Soc.* **83** (2000) 3049.
21. *Idem.*, *J. Mater. Sci.* **37** (2002) 1793.
22. K. KUMAGAWA, H. YAMAOKA, M. SHIBUYA and T. YAMAMURA, *Ceram. Eng. Sci. Proc.* **18** (1997) 113.
23. M. TAKEDA, J. SAKAMOTO, A. SAEKI, Y. IMAI and H. ICHIKAWA, *ibid.* **16** (1995) 37.
24. T. ISHIKAWA, M. SATO, S. KAJII, Y. TANAKA and M. SUZUKI, *ibid.* **22** (2001) 471.
25. B. SCHNEIDER, A. GUETTE, R. NASLAIN, M. CATALDI and A. COSTECALDE, *J. Mater. Sci.* **33** (1998) 535.
26. S. SINGHAL, *ibid.* **11** (1976) 1246.
27. M. A. LALAMLIN, F. L. ROLEY and R. L. FORDHAM, *J. Eur. Ceram. Soc.* **10** (1992) 347.

Received 13 November 2001
and accepted 3 June 2002